Gondwana Research xxx (2015) xxx–xxx

Contents lists available at ScienceDirect

Gondwana Research

journal homepage: www.elsevier.com/locate/gr

Provenance of Permian–Triassic Gondwana Sequence units accreted to the Banda Arc in the Timor region: Constraints from zircon U–Pb and Hf isotopes

Christopher J. Spencer [a,b,*], Ron A. Harris [a], Jonathan R. Major [a,c]

[a] Department of Geological Sciences, Brigham Young University, Provo, UT 84602, USA
[b] Department of Applied Geology, Curtin University, Perth, WA 6845, Australia
[c] Bureau of Economic Geology, University of Texas at Austin, Austin, TX 78713, USA

ARTICLE INFO

Article history:
Received 17 June 2015
Received in revised form 30 September 2015
Accepted 14 October 2015
Available online xxxx

Handling Editor: A.R.A. Aitken

Keywords:
Banda arc
Timor
Detrital zircons
Gondwana
Arc-continent collision

ABSTRACT

Analysis of zircons from Australian affinity Permian–Triassic units of the Timor region yield age distributions with large age peaks at 230–400 Ma and 1750–1900 Ma, which are similar to zircon age spectra found in rocks from NE Australia and crustal fragments now found in Tibet and SE Asia. It is likely that these terranes, which are now widely separated, were once part of the northern edge of Gondwana near what is now the northern margin of Australia. The Cimmerian Block rifted from Gondwana in the Early Permian during the initial formation of the Neo-Tethys Ocean. The zircon age spectra of the Gondwana Sequence of NE Australia and in the Timor region are most similar to the terranes of northern Tibet and Malaysia, further substantiating a similar tectonic affinity. A large 1750–1900 Ma zircon peak is also very common in other terranes in SE Asia.

Hf analysis of zircon from the Aileu Complex in Timor and Kisar Islands shows a bimodal distribution (both radiogenically enriched and depleted) in the Gondwana Sequence at ~300 Ma. The magmatic event from which these zircons were derived was likely bimodal (i.e. mafic and felsic). This is substantiated by the presence of Permian mafic and felsic rocks interlayered with the sandstone used in this study. Similar rock types and isotopic signatures are also found in Permian–Triassic igneous units throughout the Cimmerian continental block.

The Permian–Triassic rocks of the Timor region fill syn-rift intra-cratonic basins that successfully rifted in the Jurassic to form the NW margin of Australia. This passive continental margin first entered the Sunda Trench in the Timor region at around 7–8 Ma causing the Permo-Triassic rocks to accrete to the edge of the Asian Plate and emerge as a series of mountainous islands in the young Banda collision zone. Eventually, the Australian continental margin will collide with the southern edge of the Asian plate and these Gondwanan terranes will rejoin.

1. Introduction

Asia is an evolving supercontinent built mostly of continental fragments rifted from the former supercontinent of Gondwana (e.g. Metcalfe, 2013). Some of these fragments were rifted from what is now the passive margin of northern Australia. Petrographic and paleocurrent studies of the Gondwanan affinity sedimentary rocks of northern Australia indicate they were derived mostly from the north where continental fragments of Gondwana were subsequently rifted away (Bird, 1987; Bird and Cook, 1991; Zobell, 2007; Harris, 2011). Various paleogeographic reconstructions attach the Lhasa, Sibumasu (*Si*am–*Bu*rma–*Ma*laysia–*Su*matra), East Java and Borneo terranes to NW Australia at various times (Metcalfe, 2002; Ferrari et al., 2008; Metcalfe, 2011; Gibbons et al., 2015). This paper aims to test the veracity of these reconstructions by combining the methods of sandstone petrography and U–Pb analysis of detrital zircons to address the question of what rifted away from the NW margin of Australia.

Large sections of the strata making up the NW passive margin of Australia are accreted to the Banda Arc via Late Miocene to present arc-continent collision (i.e. Carter et al., 1976). We have analyzed petrological relations and U–Pb ages of detrital zircons from Gondwana affinity sandstones and metamorphic rocks in the Banda Arc in order to determine a provenance and age fingerprint to compare with various terranes in Asia.

2. Description of the Gondwana Sequence

Three major tectono-lithic units make up the Banda Arc collision, viz. the Banda Terrane and two sedimentary successions separated by a Late Jurassic breakup unconformity, known together as the Gondwana Sequence. The Banda Terrane consists of mostly forearc basement units of Asian affinity that form the upper plate of the collision. It occupies the highest structural level in the Banda Arc collision (Harris, 2006; Standley and Harris, 2009). Subcreted beneath the Banda Terrane is the Gondwana Sequence, which makes up the Australian passive margin

* Corresponding author at: Department of Applied Geology, Curtin University, Perth, WA 6845, Australia. Tel.: +61 8 9266 1951; fax: +61 8 9266 3153.
E-mail address: cspencer@curtin.edu.au (C.J. Spencer).

http://dx.doi.org/10.1016/j.gr.2015.10.012
1342-937X/

lower plate of the arc-continent collision (Fig. 2). Pre- and syn-breakup strata below the unconformity formed during the Pennsylvanian to Jurassic while Australia was part of Gondwana and are known as the Gondwana Mega-sequence (Audley-Charles, 1968; Harris et al., 2000; Haig et al., 2008). The Australian Passive Margin Mega-sequence overlies the unconformity.

The recent subduction of the Australian passive margin beneath the Banda Terrane caused the two mega-sequences that comprise the passive margin to detach and accrete to the upper plate. The detachment zone more or less follows the thick Wai Luli Shale immediately beneath the Jurassic breakup unconformity. The passive margin mega-sequence above the unconformity detaches at deformation front to form a classic imbricate stack (Charlton et al., 1991; Harris, 1991, 2011). The underlying Gondwana mega-sequence is carried further down the subduction zone where it eventually detaches to form a duplex system under the Banda Terrane (Harris, 1991; Harris et al., 1998).

The stratigraphy and sedimentology of Gondwana mega-sequence units in the Banda Arc are described by many previous studies dating back to early Dutch expeditions of late 19th and early 20th centuries (Rothpletz, 1891; Wanner, 1913, 1956). Other studies of these rocks include: Simons (1939), Gageonnet and Lemoine (1958), Audley-Charles (1968), Gianni (1971), Grady and Berry (1977), Charlton (1989), Bird and Cook (1991), Hunter (1993), Barkham (1993), Sawyer et al. (1993), Prasetyadi and Harris (1996), Harris et al. (1998, 2000, 2009), Charlton (2002), Charlton et al. (2009), Vorkink (2004), McCartain and Backhouse (2006), Kaneko et al. (2007), Zobell (2007), Haig et al. (2008), and Major (2011). From these studies it is evident that Gondwana Mega-sequence units exposed in the Banda Collision and drilled offshore on the Australian margin are best divided into two series, the Permian–Triassic Aileu-Maubisse Series, and the Permian–Jurassic Kekneno Series (Lemoine, 1959; Audley-Charles, 1968; Rosidi et al., 1981; Sawyer et al., 1993). The stratigraphic relationship between the two series is ambiguous due to the fact that in most places the Aileu-Maubisse series is thrust over the Kekneno Series.

2.1. Aileu Complex

The Aileu Complex is the metamorphosed part of the Aileu-Maubisse Series. It is found in several places along the north coast of Timor as far east as Manatutu (Fig. 1). It is also exposed on the island of Kisar (Richardson and Blundell, 1996; Harris, 2006; Major et al., 2013) and likely on other outer-arc islands to the east based on lithological similarities (Kaneko et al., 2007). The Aileu Complex consists of a protolith of Permian–Triassic, and possibly Jurassic, psammite and limestone, and basalt, rhyolite, tuffaceous material and gabbroic and dioritic plutons (Berry and McDougall, 1986; Prasetyadi and Harris, 1996; Harris, 2011). These units are metamorphosed into pelitic schist and gneiss, marble, phyllite and amphibolite. Metamorphic grade varies between lower greenschist to upper amphibolite facies (Berry and Grady, 1981). Some high temperature metamorphism may have occurred during the rifting event that formed the edge of the Australian continental margin. This event is overprinted by medium to high-pressure metamorphism during Late Miocene onset of collision in central Timor (Berry and McDougall, 1986; Harris, 1991; Harris et al., 2000).

2.2. Maubisse Formation

The Maubisse Formation consists of a distinct red, crinoidal limestone, shale and volcanic rocks that were deposited mostly during the Permian with ages ranging from latest Pennsylvanian to Triassic, and represents the oldest rocks exposed in the Banda Orogen (de Roever, 1940; Audley-Charles, 1968; Davydov et al., 2013). Pillow lavas found within the Maubisse Formation have geochemical signatures of within-plate and ocean-ridge basalt, which is interpreted as representing the onset of rifting (Berry and Jenner, 1982). Clastic sedimentary units found in the Maubisse Formation show fining in grain size toward the south (Carter et al., 1976). Rocks similar to the Maubisse Formation are documented on the Sahul Shoals of the undeformed Australian continental margin (Grady and Berry, 1977).

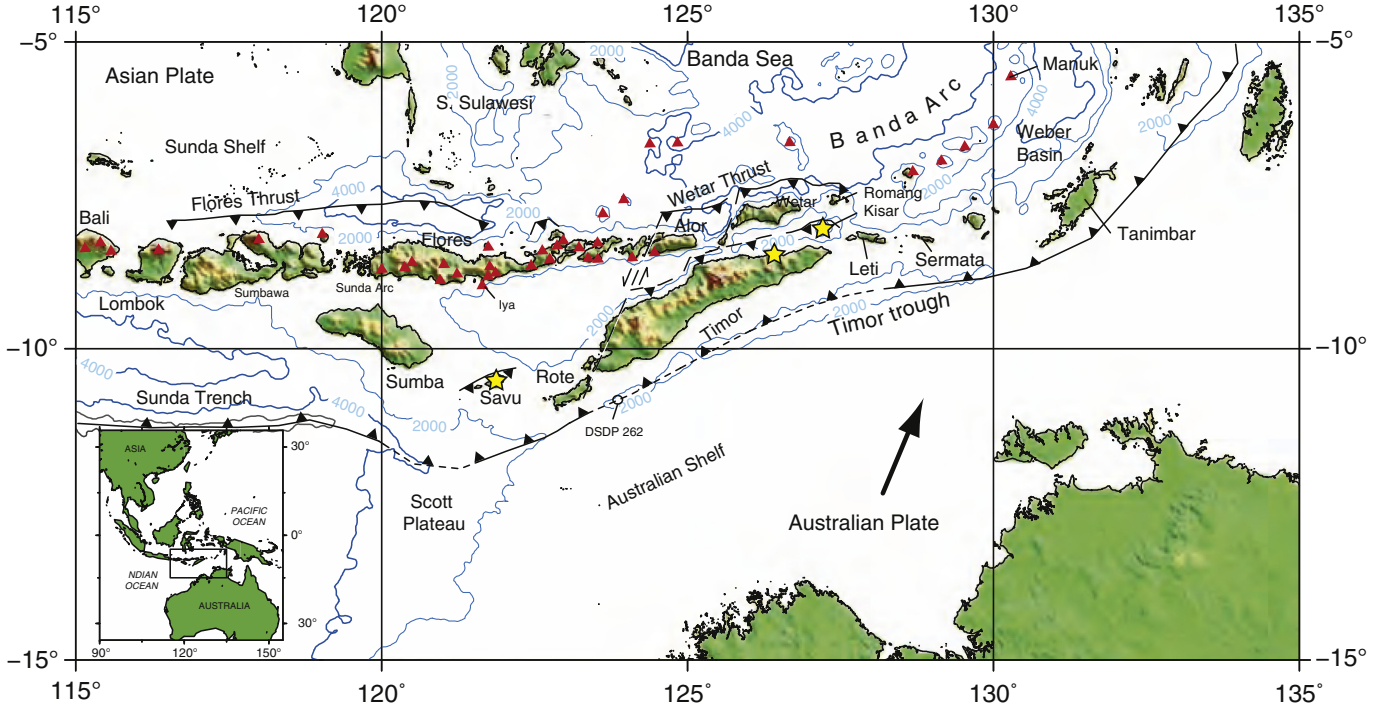

Fig. 1. Regional tectonic map of the Banda Arc region showing active faults (black, dashed if poorly defined) and active volcanoes (red triangles) (from Harris, 2011). Stars represent localities from which samples were taken. (For interpretation of the references to color in this figure legend, the reader is referred to the web version of this article.)

Please cite this article as: Spencer, C.J., et al., Provenance of Permian–Triassic Gondwana Sequence units accreted to the Banda Arc in the Timor region: Constraints from zircon U–Pb and Hf isotopes, Gondwana Research (2015), http://dx.doi.org/10.1016/j.gr.2015.10.012

2.3. Atahoc Formation

The Atahoc Formation is most likely transitional with the Maubisse Formation and is Permian in age. This formation is mainly shale with some fine-grained sandstone and volcanic rocks. The basal contact has not been found and the upper contact is amygdaloidal basalt (Sawyer et al., 1993).

2.4. Cribas Formation

The Permian–Triassic? Cribas Formation is dominated by organic shale in the lower section and inter-bedded to massive sandstone units in the upper part. This sandstone is interpreted as being part of a submarine fan complex (Hunter, 1993) deposited on a shallow shelf (Bird, 1987). Another distinguishing characteristic is the presence of ironstone nodules indicative of anoxic conditions (Charlton et al., 2002).

2.5. Niof Formation

The Triassic Niof Formation is recognized in West Timor and may comprise the upper part of the Cribas Formation in East Timor. It consists of thin, inter-bedded claystone, brown, gray and black shale, and sandstone. Bird and Cook (1991) interpreted the deposition of the Niof as turbidites in shallow to deep water. The upper portion of the Niof is interbedded with the Aitutu formation (Sawyer et al., 1993).

2.6. Aitutu Formation

The Triassic Aitutu Formation is the most distinctive unit of the Gondwana Sequence. It is a rhythmically bedded white to pink limestone with thin inter-beds of dark gray shale. The Aitutu Formation was deposited on an open marine outer shelf (Sawyer et al., 1993). It is the most lithologically distinct unit of the Kekneno Series and is used as a marker unit for structural reconstructions (Harris, 2011).

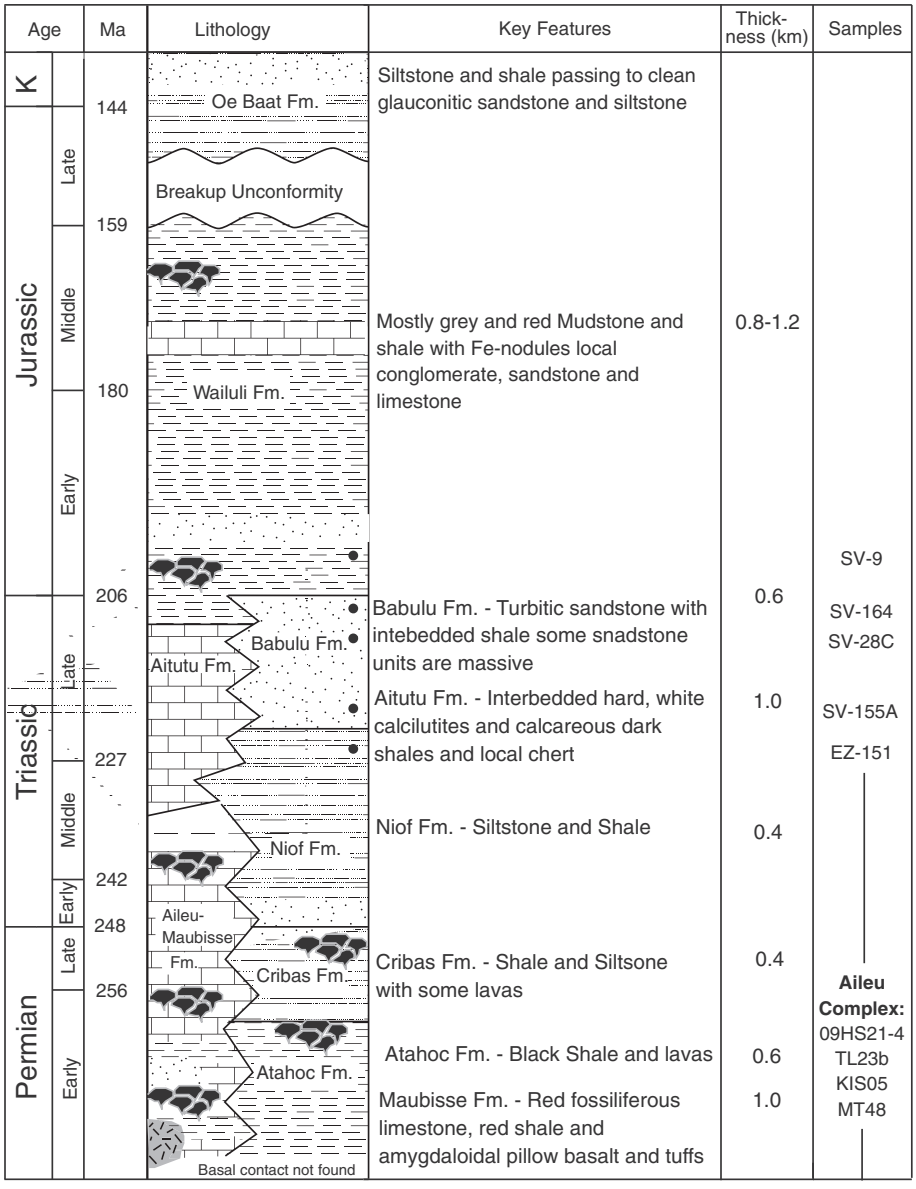

Fig. 2. Stratigraphic column of the Gondwana Sequence (after Zobell, 2007).

Please cite this article as: Spencer, C.J., et al., Provenance of Permian–Triassic Gondwana Sequence units accreted to the Banda Arc in the Timor region: Constraints from zircon U–Pb and Hf isotopes, Gondwana Research (2015), http://dx.doi.org/10.1016/j.gr.2015.10.012

Table 1
Sample age and lithologic characteristics and GPS location.

Sample	Rock unit	Lithology	Stratigraphic age	Locality	Latitude (S)			Longitude (E)			U–Pb age (Ma)	Type
					deg	min	s	deg	min	s		
KIS05	Aileu Complex	Schist	Permo-Triassic	Kisar	8	3	4.7	127	11	5.3	<300 Ma	D
MT48	Aileu Complex	Schist	Permo-Triassic	Kisar	8	1	58.5	127	10	35.4	<300 Ma	D
09HS21-4	Aileu Complex	Schist	Permo-Triassic	Timor	8	31	14.0	125	36	26.5	<300 Ma	D
TL-89	Aileu Complex	Gabbro	Permo-Carb Boundary	Timor	8	29	10.2	125	57	7.0	7.5 ± 0.4*, ~260 Ma	Ig
TL-88b	Aileu Complex	Gabbro	Permo-Carb Boundary	Timor	8	29	12.9	125	57	10.3	8.4 ± 0.57*, ~245 Ma	Ig
TL-23b	Aileu Complex	Migmatite	Permo-Carb Boundary	Timor	8	30	2.8	125	56	39.0	301 ± 3	Ig
EZ-151	Gondwana Sequence	Sandstone	Triassic	Timor	8	55	56.4	125	54	12.5	<250 Ma	D
SV-9	Gondwana Sequence	Sandstone	Triassic	Savu	10	34	48.8	121	44	32.3	<250 Ma	D
SV-28C	Gondwana Sequence	Sandstone	Triassic	Savu	10	36	5.0	121	52	3.6	<250 Ma	D
SV-164	Gondwana Sequence	Sandstone	Triassic	Savu	10	36	37.8	121	49	36.2	<250 Ma	D
SV-159	Gondwana Sequence	Sandstone	Triassic	Savu	10	33	6.4	121	51	32.0	<250 Ma	D
SV-155A	Gondwana Sequence	Sandstone	Triassic	Savu	10	36	35.1	121	51	40.1	<250 Ma	D

D: minimum depositional age based upon 2nd youngest zircon.
Ig: weighted average.
* Metamorphic age.

2.7. Babulu Formation

The Triassic Babulu Formation is only recognized in central Timor (Gianni, 1971; Bird and Cook, 1991) and Savu (Vorkink, 2004), and may comprise the base of the Wai Luli Formation in East Timor. The Babulu Formation consists of sandstone, shale and silts with some massive sandstone beds. Deposition of this unit most likely occurred in a proximal near shore to shelf break (Sawyer et al., 1993) through turbidity currents from a prograding delta (Bird and Cook, 1991).

2.8. Wai Luli Formation

The Late Triassic to Jurassic Wai Luli Formation is a thick succession of mostly smectite-rich mudstone (Harris et al., 1998) with some well-bedded marl, calcilutite, micaceous shale and quartz arenite. Toward the top of the formation are conglomerate and red shale units (Audley-Charles, 1968). Ironstones are very common and form lag deposits on the surface. In the Banda collision zone the thick, mechanically weak Wai Luli mudstone serves as a major decollement for imbrication of the overlying Australian Passive Margin Sequence; and as a roof thrust for structural duplexes of the Gondwana Sequence (Harris, 1991). It also is the source of much of the mélange matrix found along the suture zone between accreted Australian continental material and structurally overlying Asian affinity arc terranes (Harris et al., 1998).

3. Methods

The source regions for Gondwana Sequence sandstones were also investigated by petrographic studies of grain types and textures, and U–Pb age analyses of detrital zircon grains. The petrographic analysis (reported in Zobell, 2007) includes 16 samples of Triassic Gondwana Sequence sandstone collected from Savu, West Timor and East Timor.

U–Pb zircon age and Hf analyses were conducted on 5 sandstone and 4 metamorphic rock samples from Savu, Timor and and Kisar (Fig. 2). These samples were crushed using a jaw crusher and the <500 μm size fraction was magnetically separated using the Carpco and Frantz

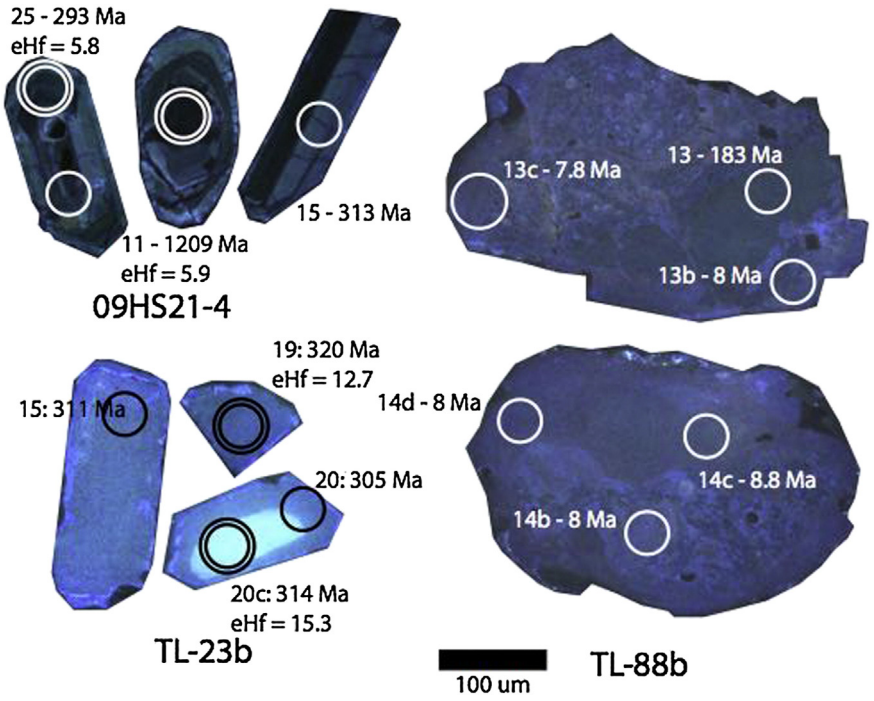

Fig. 3. Cathode luminescence (CL) image of zircon with outline of typical U–Pb (40/50 μm), and Hf (50 μm) analytical spots.

Please cite this article as: Spencer, C.J., et al., Provenance of Permian–Triassic Gondwana Sequence units accreted to the Banda Arc in the Timor region: Constraints from zircon U–Pb and Hf isotopes, Gondwana Research (2015), http://dx.doi.org/10.1016/j.gr.2015.10.012

magnetic separators. Heavy minerals were separated using wifely table and/or tetraboroethelene. Zircon grains were then handpicked for analysis. Cathode luminescence and backscatter images were acquired using a Hitachi 3400N SEM/Catan Chroma CL system and a Cameca SX-50 electron microprobe, respectively.

In situ U–Pb isotope analyses for individual grains were performed using a Nu Plasma HR MC-ICPMS coupled to a New Wave 193 nm ArF and a Photon Machines G3 193 nm ArF laser ablation system at the University of Arizona with ablation done in a He carrier gas using a 40 μm diameter spot size. Laser fluence of ~4 J/cm^2 at 8 Hz for 30 s of integration. Detailed U–Pb analytical procedures are described by Gehrels et al. (2008). Samples were analyzed in sets of 9 to 12 analyses, which include 5 to 8 unknown spots, bracketed beginning and end by a pair of analyses of an in house Sri Lanka zircon standard (Gehrels et al., 2008). The R33 zircon standard was also analyzed at the beginning and end of each sample set as an independent control on reproducibility and instrument stability. Concordance is defined for ages above 700 Ma using the ratio of $^{206}Pb/^{238}U$ and $^{207}Pb/^{206}Pb$ ages, and $^{206}Pb/^{238}U$ and $^{207}Pb/^{235}U$ ages are used for those younger than 700 Ma. The accepted ages were selected from a 95% concordant subset, wherein the $^{206}Pb/^{238}U$ and $^{207}Pb/^{206}Pb$ ages are used for zircons younger and older than 700 Ma, respectively; this age was chosen because there is a natural gap in the ages of the zircons in these samples. Visualization of U–Pb

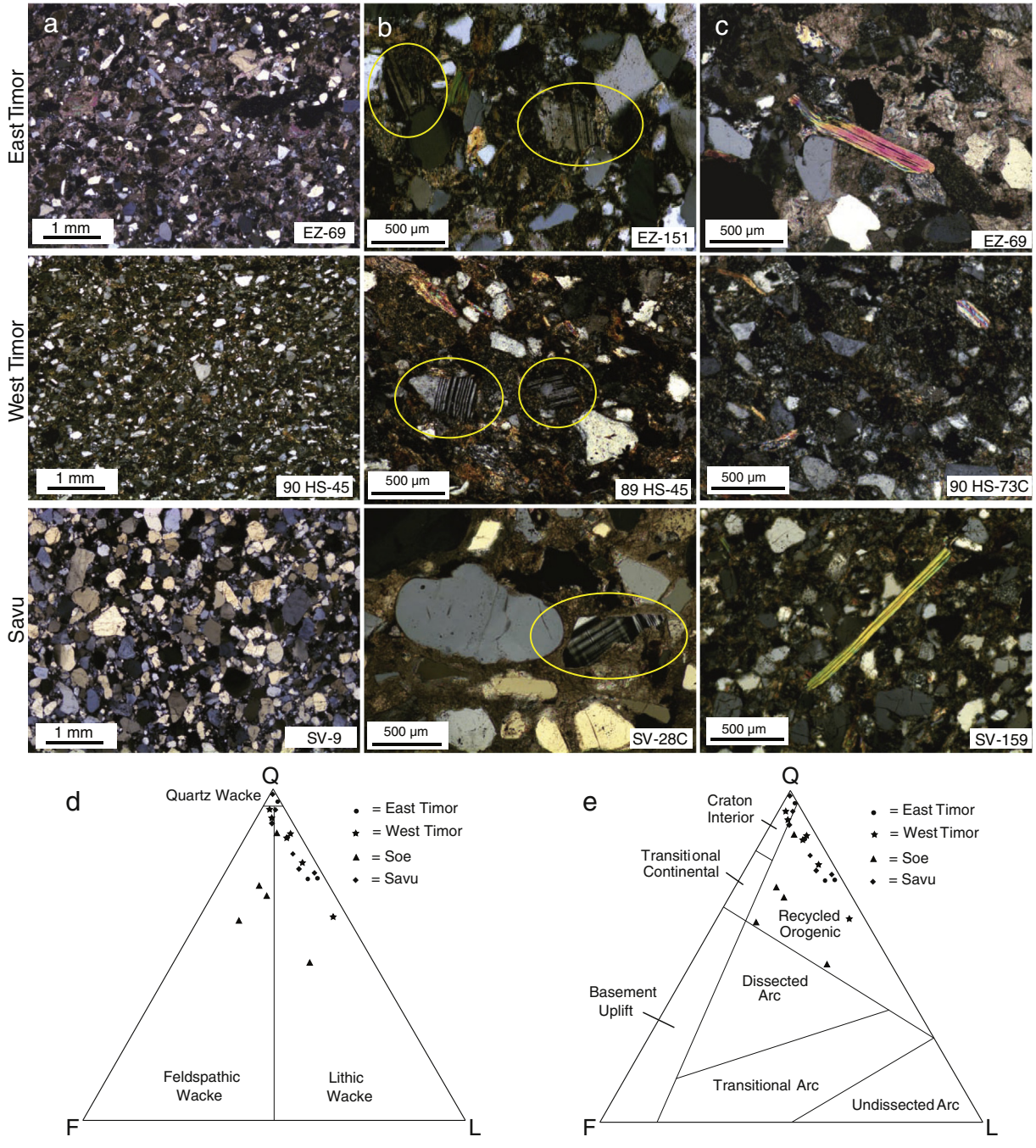

Fig. 4. Column a) photomicrographs in cross polarized light showing sub-angular to sub-rounded sandstone textures of representative Triassic Gondwana sequence sandstone from East and West Timor and Savu. b) Photomicrographs in cross polarized light of unaltered twinned feldspar grains (circled). c) Photomicrographs in cross polarized light of fresh micas. d) QFL diagram of Williams et al. (1982) for classification of sandstone samples from the Triassic Gondwana Sequence. e) QFL sedimentary provenance based on Dickinson et al. (1983). Photomicrographs and point counting data are from Zobell (2007).

Please cite this article as: Spencer, C.J., et al., Provenance of Permian–Triassic Gondwana Sequence units accreted to the Banda Arc in the Timor region: Constraints from zircon U–Pb and Hf isotopes, Gondwana Research (2015), http://dx.doi.org/10.1016/j.gr.2015.10.012

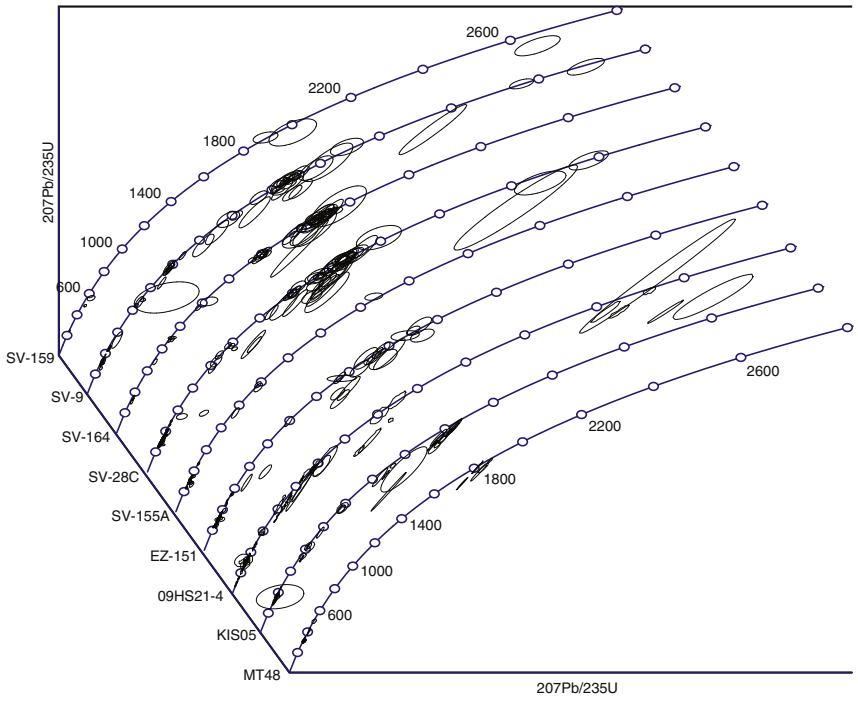

Fig. 5. Pb/U concordia diagram of zircon analyses from each sample constructed using Isoplot 4.15 (Ludwig, 2003). Uncertainties are shown at the 2σ level.

concordia and zircon ages is achieved using Isoplot 4.15 (Ludwig, 2003) and densityplotter (Vermeesch, 2012). GPS locations of samples are presented in Table 1.

Hf isotope analyses were performed with a Nu Plasma HR MC-ICPMS coupled to a Photon Machines G3 193 nm ArF laser ablation system. Instrument settings were established first by analysis of 10 ppb solutions of JMC475 and a Spex Hf solution, and then by analysis of 10 ppb solutions containing Spex Hf, Yb, and Lu. The mixtures range in concentration of Yb and Lu, with ^{176}(Yb + Lu) up to 70% of the ^{176}Hf. When all solutions yield an accurate ^{176}Hf/^{177}Hf ratio, instrument settings are optimized for laser ablation analyses and seven different standard zircons (Mud Tank, 91500, Temora, R33, FC52, Plesovice, and Sri Lanka) are analyzed. These standards are included with unknowns on the same epoxy mounts. Laser ablation analyses were conducted with a laser beam diameter of 50 μm, with ablation pits located on top of the U–Pb analysis pits or on an adjacent spot of similar zonation. CL images were used to ensure that the ablation pits do not overlap multiple age domains or inclusions (Fig. 3). Each acquisition consisted of one 40-second integration on backgrounds (on peaks with no laser firing) followed by 60 one-second integrations with the laser firing. Using a typical laser fluence of ~5 J/cm^2 and pulse rate of 7 Hz. Sets of each standard was analyzed once for every ~15 unknowns.

Isotope fractionation was accounted for using the method of Woodhead et al. (2004): βHf is determined from the measured ^{179}Hf/^{177}Hf; βYb is determined from the measured ^{173}Yb/^{171}Yb (except for very low Yb signals); βLu is assumed to be the same as βYb; and an exponential formula is used for fractionation correction. Yb and Lu interferences were corrected by measurement of ^{176}Yb/^{171}Yb and ^{176}Lu/^{175}Lu (respectively), as advocated by Woodhead et al. (2004). Critical isotope ratios are ^{179}Hf/^{177}Hf = 0.73250 (Patchett and Tatsumoto, 1980); ^{173}Yb/^{171}Yb = 1.132338 (Vervoort et al. 2004); ^{176}Yb/^{171}Yb = 0.901691 (Vervoort et al., 2004; Amelin and Davis, 2005); ^{176}Lu/^{175}Lu = 0.02653 (Patchett, 1983). All corrections are done line-by-line. For very low Yb signals, βHf is used for fractionation of Yb isotopes. The corrected ^{176}Hf/^{177}Hf values are filtered for outliers (2-sigma filter), and the average and standard error are calculated from the resulting ~58 integrations. There is no capability to use only a portion of the acquired data.

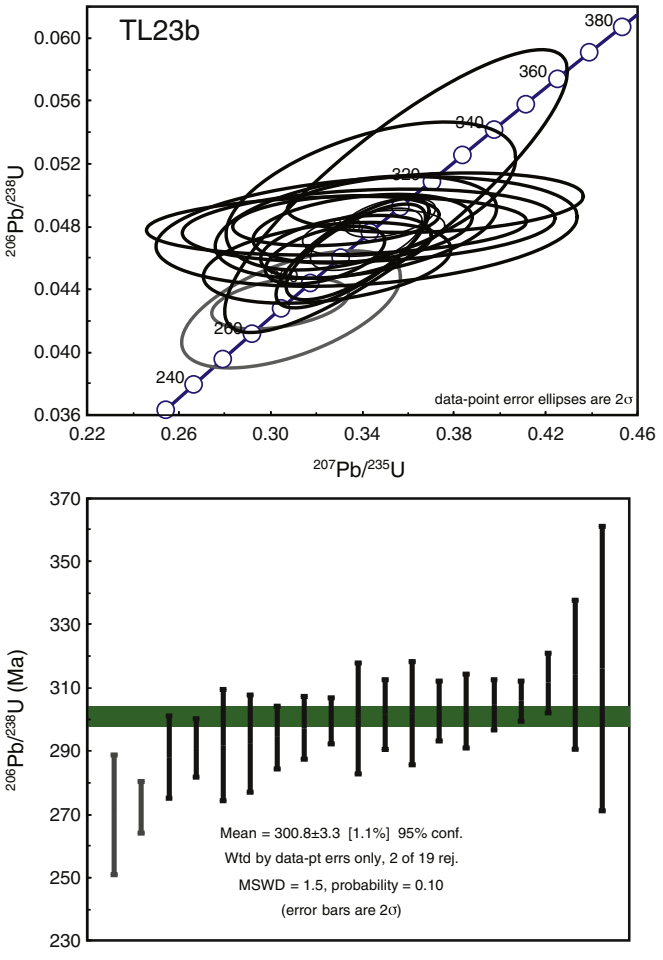

Fig. 6. Top: Pb/U concordia diagram of zircon analyses for sample TL23b. Bottom: weighted mean diagram of the same. The youngest two analyses in gray were discarded as they fall outside the 2-sigma envelope and likely represent Pb-loss.

Please cite this article as: Spencer, C.J., et al., Provenance of Permian–Triassic Gondwana Sequence units accreted to the Banda Arc in the Timor region: Constraints from zircon U–Pb and Hf isotopes, Gondwana Research (2015), http://dx.doi.org/10.1016/j.gr.2015.10.012

The $^{176}Hf/^{177}Hf$ at time of crystallization is calculated from measurement of present-day $^{176}Hf/^{177}Hf$ and $^{176}Lu/^{177}Hf$, using the decay constant of ^{176}Lu ($\lambda = 1.867e-11$) from Scherer et al. (2001) and Söderlund et al. (2004). The uncertainty propagation of the epsilon notation also includes the uncertainty of the $^{207}Pb/^{206}Pb$ crystallization age, as it is time integrated. Although this may be an over propagation of uncertainty, we prefer this conservative approach for the epsilon notation when defining specific fields of similar εHf compositions. Uncertainties that incorporate the crystallization age uncertainty are on average 50% ($1\sigma = 20\%$) larger than uncertainties that do not consider the crystallization age uncertainty.

4. Results

4.1. Petrography

Point count analysis of Gondwana Sequence sandstones from Savu and West and East Timor (initially reported by Zobell, 2007) indicates that they are quartz wackes to lithic wackes (Fig. 4a) on the classification diagram of Williams et al. (1982). On discrimination diagrams of Dickinson et al. (1983) the sandstones plot as recycled orogen provenance (Fig. 4b). In terms of texturally maturity the sandstones we analyzed are immature, and are characterized by large, sub-angular to sub-rounded framework grains (Fig. 4c). Immaturity is also indicated by significant amounts of unaltered twinned feldspar (Fig. 4d), fresh mica (Fig. 4e), lithic fragments, and high percentages of matrix. These data preclude a far-traveled source for most of the detrital zircons.

4.2. Zircon U–Pb analysis

Zircons were separated in 5 sandstone and 4 metamorphic rock samples of the Gondwana Sequence in the Timor region. These zircon grains provide the first constraints for depositional provenance and maximum age of deposition for various sections of the Gondwana Sequence (Table 1). Four of these samples are from Triassic units exposed on the island of Savu (Indonesia), one is from Triassic sandstone in East Timor and the other four are from the Aileu Complex in East Timor and Kisar Island (see Fig. 2). Most of the grains are amber to clear or pink to mauve in color with variable amounts of abrasion and rounding. Proterozoic zircons vary in color, but Paleozoic zircons are only amber to clear. Both abraded and pristine zircons are present, although there is no apparent relationship between abrasion and age. Zircons from nine samples are variably concordant (Figs. 5 and 6) and those that are <5% discordant cluster into two main populations at ~300 Ma and

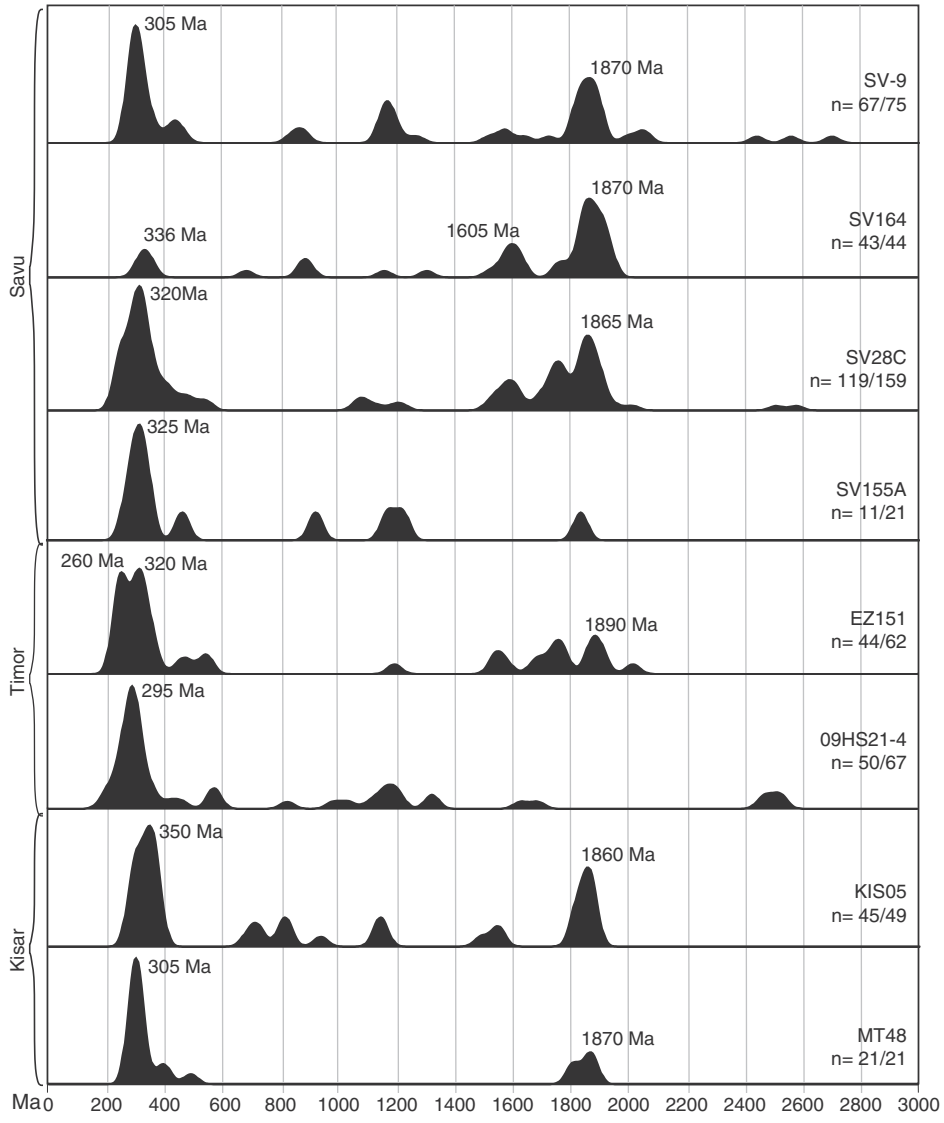

Fig. 7. Kernel density estimation (solid line) plots of detrital zircon ages from each sample. Only ages that <5% discordant are used. Plot is constructed using densityplotter (Vermeesch, 2012).

Please cite this article as: Spencer, C.J., et al., Provenance of Permian–Triassic Gondwana Sequence units accreted to the Banda Arc in the Timor region: Constraints from zircon U–Pb and Hf isotopes, Gondwana Research (2015), http://dx.doi.org/10.1016/j.gr.2015.10.012

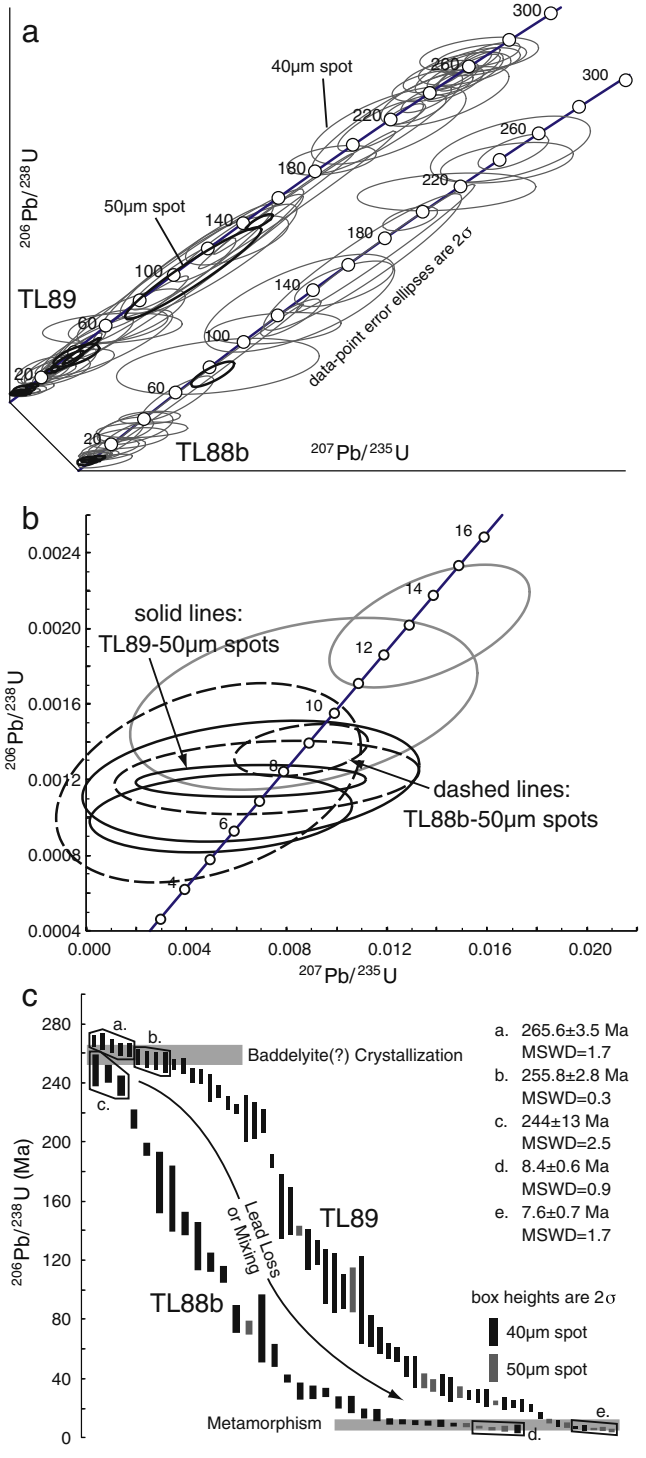

Fig. 8. a) Pb/U concordia diagram of ages (Ma) of zircon grains from samples TL89 and TL88b constructed with the use of Isoplot (Ludwig, 2003). Uncertainties are shown at the 2σ level. 40 and 50 μm spots are displayed in gray and black, respectively. b) Pb/U concordia diagram of ages (Ma) of the youngest zircon ages analyzed with 50 μm spots. Concordia ages from the youngest three analyses. Gray analyses are not included in the concordia age calculation. c) Zircon ^{206}Pb/^{238}U age analyses plotted with 2σ uncertainties. The oldest plateau of ages represents the crystallization of a primary U-bearing phase in gabbroic rocks (possibly baddeleyite) and the youngest plateau represents the age of metamorphic zircon growth whereas the zircon analyses with between these two events represent varying degrees of lead loss. 40 and 50 μm spots are displayed in black and gray, respectively. Analyses within polygons (a) through (e) correspond to weighted averages of three to five analyses that broadly represent the igneous and metamorphic crystallization events.

~1875 Ma (Fig. 7). Several other small peaks are found in some grains between these two age groups. The peak at ~300 Ma includes a spread of discordant ages from mid-Carboniferous to Jurassic (~330 to 150 Ma).

Sample TL23b was collected from a leucosome pod within a migmatitic unit in the Aileu Complex. Zircons within this leucosome (17/19 analyses) give a weighted average of 300.8 ± 3.3 Ma (MSWD = 1.5) (Fig. 6). This age implies that there was partial melting associated with the rifting episode in this region, although there is no evidence of partial melting during the Miocene collision of Australia (see also Berry and Grady, 1981).

Two amphibolite samples (TL89, TL88b) from the Aileu Complex were analyzed using both 40 μm and 50 μm diameter spots. Both sets of data reveal a suite of ages between ~300 Ma and ~7 Ma that lie along a poorly defined discordia. The weighted averages of oldest clusters of ages whose ^{206}Pb/^{238}U and ^{207}Pb/^{235}U uncertainties overlap with the concordia are 266 ± 4 (n = 5; MSWD = 1.7) and 256 ± 3 (n = 4; MSWD = 0.33) (^{206}Pb/^{238}U age) in sample TL88b and 269 ± 4 and 244 ± 13 (n = 3; MSWD = 2.5) in sample TL89 (Fig. 8).

4.3. Hf analysis

Hf isotopic analyses of three detrital zircon samples from Kisar (KIS05 and MT4891) and Timor (09-HS21-4) have initial εHf values of 11 to −21 (Fig. 9). The pre-400 Ma zircons have εHf values of 5 to −10 whereas post-400 Ma zircons have only subchondritic εHf values.

Very young zircons (~7 Ma) from amphibolite samples (TL88b, TL89) have initial εHf values of 4.2 to −2.3 although this is likely a

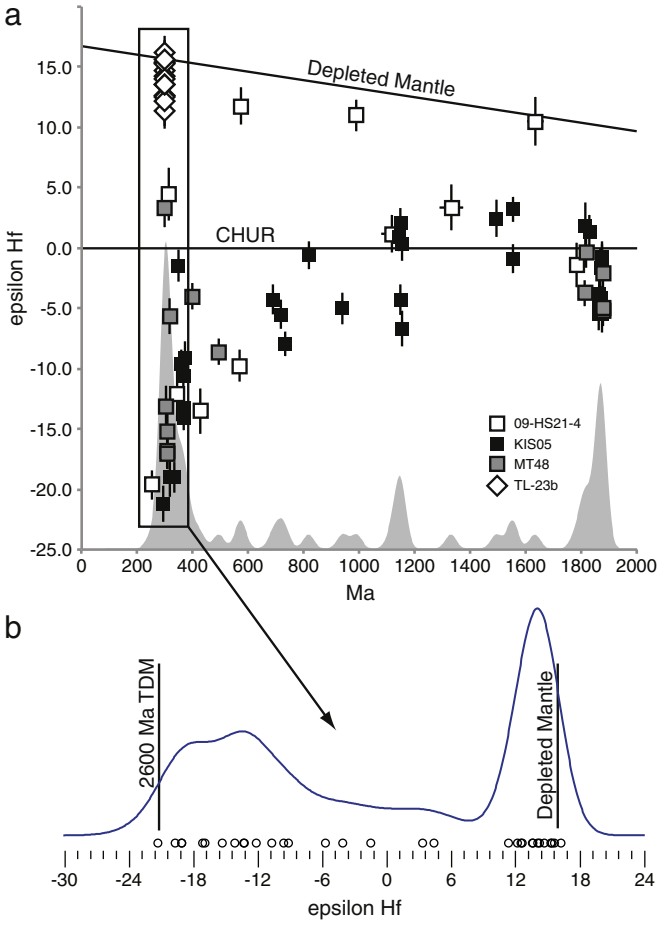

Fig. 9. a) $\varepsilon Hf_{(t)}$ vs. U–Pb analyses of detrital zircons from the samples in this study. Uncertainties are displayed as 2σ. DM = depleted mantle. b) KDE of εHf from the youngest set of zircon ages displaying a bimodal distribution.

maximum estimate given the potential for lead loss in the ages used to calculate the initial εHf. Hf isotopic analyses of zircon grains from the Aileu Complex migmatite (sample TL23b) have initial εHf values of 11 to 16.

5. Discussion

5.1. Provenance of the Gondwana Sequence

Samples of the Gondwana Sequence on the islands of Savu, Timor, and Kisar have dominant zircon U–Pb age peaks at ~300 and ~1875 Ma with minor Neoproterozoic to Archean subpopulations (Fig. 7). The ~1875 Ma population was likely derived from the North Australian Craton within the Kimberly Basin, and Halls Creek and Pine Creek orogens (Tyler et al., 2005; Downes et al., 2007; Worden et al., 2008; Lewis and Sircombe, 2013). Additionally, the few pre-2.4 Ga detrital zircons were also likely derived from the North Australian Craton (Downes et al., 2007; Cawood and Korsch, 2008). Potential sources for the few Meso- to Neoproterozoic detrital zircons have been identified within the Musgrave Province, Albany-Fraser Orogen, and Pinjarra Orogen of central and western Australia. The presence of zircons from Western Australia was likely transported along the west and north coast prior to convergence with the Pacific Plate (Lewis and Sircombe, 2013). However, it should be noted that the proportions of Meso- and Paleo-Proterozoic zircons seen along coastal Western Australia and the northwest Australian Shelf do not match that of the samples from Savu, Timor, and Kisar. The mismatch in zircon age populations might reflect a different provenance than proposed or idiosyncrasies that would be resolved with a greater number of analyses. It should be further noted, that despite the inclusion of potentially far traveled detrital

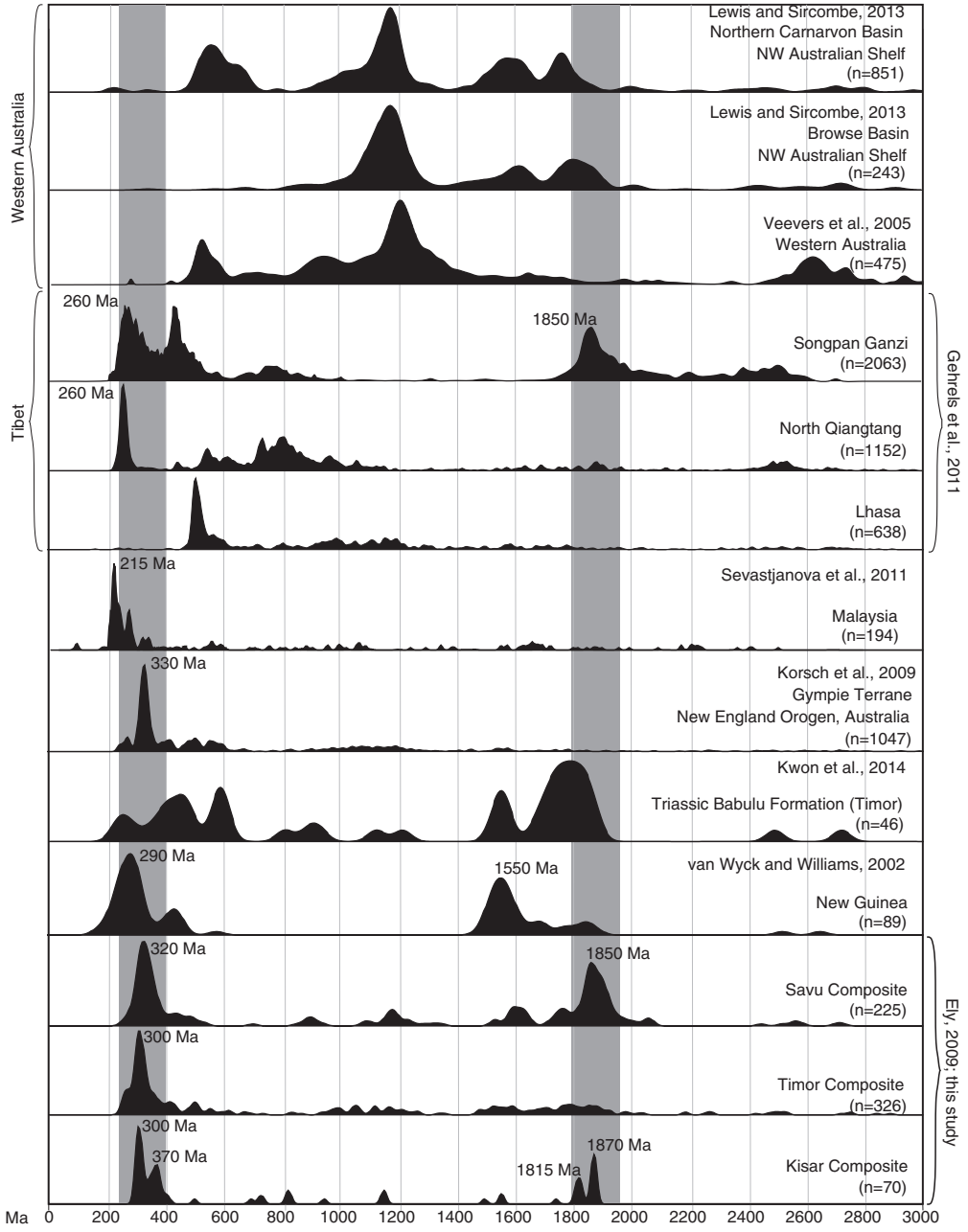

Fig. 10. Kernel density estimation (solid line) plots of composite detrital zircon age spectra from potential source regions. Data compiled from: van Wyck and Williams, 2002; Veevers et al., 2005; Zobell, 2007; Korsch et al., 2009; Sevastjanova et al., 2011; Gehrels et al., 2011; Ely et al., 2013; Kwon et al., 2014; this study. Plot is constructed using densityplotter (Vermeesch, 2012).

Please cite this article as: Spencer, C.J., et al., Provenance of Permian–Triassic Gondwana Sequence units accreted to the Banda Arc in the Timor region: Constraints from zircon U–Pb and Hf isotopes, Gondwana Research (2015), http://dx.doi.org/10.1016/j.gr.2015.10.012

zircon populations, the presence of sub-angular grain fragments along with pristine mica flecks indicate that any far-traveled detrital zircon populations were reworked along a rift shoulder and deposited in a proximal basin.

Paleoproterozoic zircon grains, with minor modes at 1.8 to 1.9 Ga, are found in nearly every sample. Smaller population of Neo- and Mesoproterozoic are also present and three of the samples (SV-9, SV28C, 09HS21-4) also contain minor Archean (~2.5 Ga) grains. The early Permian maximum depositional age of the Aileu Formation inferred by the youngest detrital zircon age peak (~300 Ma) is consistent with that proposed by Brunnschweiler (1978), who reported Permian ammonite fossils in phyllitic rocks.

Zircons in amphibolite samples TL88b and TL89 show incomplete lead loss from ~260 Ma to ~7 Ma (Fig. 8). Based upon the mafic nature of these samples and the incomplete replacement of the zircon, we postulate the cores of these grains were initially baddeleyite hosted in gabbro, which was replaced by zircon during ~7 Ma collision-related metamorphism and the influx of Si-rich fluids. Although the zircons also have elevated U/Th ratios (3.1 average) recent studies imply that the U/Th ratio of recrystallized zircon primarily reflects the composition of the fluids responsible for driving the recrystallization (Harley et al., 2007 and references therein). Alternatively, these Permian-age cores are simply heavily altered zircon with a pristine oscillatory zoned zircon rims. It is likely the mafic protolith for the amphibolite is a gabbro as argued from faint primary igneous textures. We interpret this unit as having been emplaced along the shoulder of a rift resulting from the Permian separation of the Cimmerian block from Gondwana.

Hf isotopes in the detrital zircon samples display variable radiogenic enrichment with average Paleoproterozoic to Neoarchean depleted mantle model ages (Fig. 9). An exception to this is seen in the apparent bimodal distribution of εHf values in the ~300 Ma dominant age peak. The end members of this bimodal distribution lie at the +16 and −22, which correspond to the depleted mantle and a depleted mantle model age of ~2600 Ma, respectively. This unique distribution implies that these zircons were derived from a bimodal magmatic suite, which likely formed during rifting.

Evidence for this bimodal magmatic event is seen in the Gondwana Sequence where minor amounts of rhyolite and granite are accompanied by larger volumes of alkali basalt (Audley-Charles, 1968; Wopfner and Jin, 2009). These compositions typify continental rifting events (McKee, 1970). Furthermore, the ~260 Ma upper intercept age of the metagabbro samples in this study is similar to the 255 ± 39 Ma apatite fission track age of Maubisse tuff (Harris et al., 2000) and 270 ± 3 Ma zircon U–Pb age of Maubisse Trachyandesite (Kwon et al., 2014) that may represent the same suite of bimodal volcanic rocks associated with the rifting of the Cimmerian block.

A comparison of the detrital zircon age spectra from the Gondwana Sequence of Savu, Timor, and Kisar with detrital zircon age spectra from regions in Australia and Asia provide important context for potential localities from which zircons may have been derived (Fig. 10). Importantly, the sedimentary basins of the NW Australian Shelf are the most proximal to the Banda Arc and yet show very different age spectra implying significantly different provenance (Lewis and Sircombe, 2013). In Tibet, the Songpan Ganzi Terrane shows a strong 1850 Ma population similar to that of the Gondwana Sequence, but lacks the strong 300–370 Ma age peak (Gehrels et al., 2011). Similarly, detrital zircons from the Malay peninsula have a dominant age peak younger than that of the Gondwana Sequence (Sevastjanova et al., 2011). The 300–370 Ma age population seen in the Gondwana Sequence is most similar to the rocks of the New England Orogen in NE Australia and New Guinea (van Wyck and Williams, 2002; Korsch et al., 2009); however Paleoproterozoic zircon ages are conspicuously absent from these regions and appear to have an Asian affinity relating to Sibumasu (see Wang et al., 2014; Gardiner et al., 2015).

Our story of the Gondwana Sequence comes full circle when the final remnants of the Tethys Ocean close and the Gondwana Sequence is both subducted beneath and accreted to the Banda Arc (Harris et al., 2000; Harris, 2006, 2011). Zircons from the meta-gabbros in this study have imprecisely constrained the metamorphism associated with this event at ~7 Ma (Fig. 10).

6. Conclusions

From the data presented in this study, we find that:

1. The Permian–Triassic Gondwana Sequence was deposited in intracratonic basins of Gondwana during the early breakup stage of Australian passive continental margin development.
2. These sediments, with the accompanying bimodal volcanism, represent proximal rift shoulder deposits that were lain down shortly after the initiation of Tethys Ocean rifting in the early Permian era and are now present in exhumed thrust sheets accreted to the Banda Arc complex.
3. Sandstone of the Gondwana Sequence is mostly immature and was derived predominantly from rocks to the north of the Australia that may correlate with fragments of the Cimmerian Block found in Tibet and SE Asia.
4. Zircons in meta-gabbro provide age estimates for both the rifting of Cimmeria from Gondwana in the grain cores (~300 Ma) as well as the collision of the Banda Arc with Australia (~7 Ma).
5. εHf of detrital zircons provides evidence for bimodal rift-related magmatism with one cluster of data near the depleted mantle and another with Neoarchean depleted mantle model ages.

Acknowledgments

This project was funded by the US National Science Foundation (NSF EAR-0337221 to R.H.), the College of Physical and Mathematical Sciences at Brigham Young University, and a BYU Graduate Research Fellowship (to J.M.). Michael Vorkink, and Elizabeth (Zobell) Ruiz provided some samples and analyses for this paper from their MSc. Thesis research in the Banda Arc. Gratitude is also expressed to George Gehrels, Mark Pecha, and Nicky Giesler who facilitated the analytical work at the University of Arizona Laserchron lab (NSF EAR-0929777 and NSF EAR-0443387). We appreciate the help of Carl Hoiland and Josh Flores with the analytical work.

Appendix A. Supplementary data

Supplementary data to this article can be found online at http://dx.doi.org/10.1016/j.gr.2015.10.012.

References

Amelin, Y., Davis, W.J., 2005. Geochemical test for branching decay of ^{176}Lu. Geochimica et Cosmochimica Acta 69, 465–473. http://dx.doi.org/10.1016/j.gca.2004.04.028.
Audley-Charles, M., 1968. The Geology of Portuguese Timor. Memoirs. Geological Society of London. http://dx.doi.org/10.1144/GSL.MEM.1968.004.01.02.
Barkham, S.T., 1993. The Structure and Stratigraphy of the Permo-Triassic Carbonate Formations of West Timor, Indonesia. University of London, Royal Holloway.
Berry, R.F., Grady, A.E., 1981. Deformation and metamorphism of the Aileu Formation, north coast, East Timor and its tectonic significance. Journal of Structural Geology 3, 143–167. http://dx.doi.org/10.1016/0191-8141(81)90011-0.
Berry, R., Jenner, G., 1982. Basalt geochemistry as a test of the tectonic models of Timor. Journal of the Geological Society of London 139, 593–604.
Berry, R., McDougall, I., 1986. Interpretation of ^{40}Ar/^{39}Ar and K/Ar dating evidence from the Aileu Formation, East Timor, Indonesia. Chemical Geology: Isotope Geoscience Section 59, 43–58. http://dx.doi.org/10.1016/0168-9622(86)90056-4.
Bird, P.R., 1987. The Geology of the Permo-Triassic Rocks of Kekneno, West Timor. University of London, Royal Holloway.
Bird, P.R., Cook, S.E., 1991. Permo-Triassic successions of the Kekneno area, West Timor: implications for palaeogeography and basin evolution. Journal of Southeast Asian Earth Sciences 6, 359–371. http://dx.doi.org/10.1016/0743-9547(91)90081-8.
Brunnschweiler, R.O., 1978. Notes on the geology of eastern Timor. Bulletin. Bureau of Mineral Resources. Geology and Geophysics Australia 192, 9–18.

Carter, D.J., Audley-Charles, M.G., Barber, A.J., 1976. Stratigraphical analysis of island arc—continental margin collision in eastern Indonesia. Journal of the Geological Society of London 132, 179–198. http://dx.doi.org/10.1144/gsjgs.132.2.0179.

Cawood, P.a., Korsch, R.J., 2008. Assembling Australia: Proterozoic building of a continent. Precambrian Research 166, 1–35. http://dx.doi.org/10.1016/j.precamres.2008.08.006.

Charlton, T.R., 1989. Stratigraphic correlation across an arc-continent collision zone: Timor and the Australian Northwest Shelf. Australian Journal of Earth Sciences 36, 263–274.

Charlton, T.R., 2002. The structural setting and tectonic significance of the Lolotoi, Laclubar and Aileu metamorphic massifs, East Timor. Journal of Asian Earth Sciences 20, 851–865. http://dx.doi.org/10.1016/S1367-9120(01)00075-X.

Charlton, T.R., Barber, A.J., Harris, R.A., Barkham, S.T., Bird, P.R., Archbold, N.W., Morris, N.J., Nicoll, R.S., Owen, H.G., Owen, R.M., Sorauf, J.E., Taylor, P.D., Webster, G.D., Whittaker, J.E., 2002. The Permian of Timor; stratigraphy, palaeontology and palaeogeography. Journal Asian Earth Science 20 (6), 719–774.

Charlton, T., Barber, A., Barkham, S., 1991. The structural evolution of the Timor collision complex, eastern Indonesia. Journal of Structural Geology 13, 489–500. http://dx.doi.org/10.1016/0191-8141(91)90039-L.

Charlton, T.R., Barber, A.J., McGowan, A.J., Nicoll, R.S., Roniewicz, E., Cook, S.E., Barkham, S.T., Bird, P.R., 2009. The Triassic of Timor: lithostratigraphy, chronostratigraphy and palaeogeography. Journal of Asian Earth Sciences 36, 341–363. http://dx.doi.org/10.1016/j.jseaes.2009.06.004.

Davydov, V.I., Haig, D.W., McCartain, E., 2013. A latest Carboniferous warming spike recorded by a fusulinid-rich bioherm in Timor Leste: implications for East Gondwana deglaciation. Palaeogeography, Palaeoclimatology, Palaeoecology 376, 22–38. http://dx.doi.org/10.1016/j.palaeo.2013.01.022.

de Roever, W.P., 1940. Geological investigation in the South western Moetis region (Netherlands Timor) Ph.D. Thesis, University of Amsterdam 244 pp.

Dickinson, W.R., Beard, L.S., Brakenridge, G.R., Erjavec, J.L., Ferguson, R.C., Inman, K.F., Knepp, R.A., Lindber, F.A., Ryberg, P.T., 1983. Provenance of North American Phanerozoic sandstones in relation to tectonic setting. Geological Society of America Bulletin 94, 222–235.

Downes, P.J., Griffin, B.J., Griffin, W.L., 2007. Mineral chemistry and zircon geochronology of xenocrysts and altered mantle and crustal xenoliths from the Aries micaceous kimberlite: constraints on the composition and age of the central Kimberley Craton, Western Australia. Lithos 93, 175–198. http://dx.doi.org/10.1016/j.lithos.2006.06.005.

Ely, K.S., Sandiford, M., Phillips, D., Boger, S.D., 2013. Detrital zircon U–Pb and $^{40}Ar/^{39}Ar$ hornblende ages from the Aileu Complex, Timor-Leste: provenance and metamorphic cooling history. Journal of the Geological Society of London 171, 299–309. http://dx.doi.org/10.1144/jgs2012-065.

Ferrari, O.M., Hochard, C., Stampfli, G.M., 2008. An alternative plate tectonic model for the Palaeozoic–Early Mesozoic Palaeotethyan evolution of Southeast Asia (Northern Thailand–Burma). Tectonophysics 451, 346–365. http://dx.doi.org/10.1016/j.tecto.2007.11.065.

Gageonnet, R., Lemoine, M., 1958. Contribution a la connaissance de la geologie de la province Porugaise de Timor. Monograph, Portugal, Ministerio Ultramar, Est. 48.

Gardiner, N.J., Searle, M.P., Morley, C.K., Whitehouse, M.P., Spencer, C.J., Robb, L.J., 2015. The closure of Palaeo-Tethys in Eastern Myanmar and Northern Thailand: New insights from zircon U–Pb and Hf isotope data. Gondwana Research. http://dx.doi.org/10.1016/j.gr.2015.03.001.

Gehrels, G., Kapp, P., Decelles, P., Pullen, A., Blakey, R., Weislogel, A., Ding, L., Guynn, J., Martin, A., McQuarrie, N., Yin, A., 2011. Detrital zircon geochronology of pre-Tertiary strata in the Tibetan-Himalayan orogen. Tectonics 30. http://dx.doi.org/10.1029/2011TC002868.

Gehrels, G.E., Valencia, V.a., Ruiz, J., 2008. Enhanced precision, accuracy, efficiency, and spatial resolution of U–Pb ages by laser ablation-multicollector-inductively coupled plasma-mass spectrometry. Geochemistry, Geophysics, Geosystems 9. http://dx.doi.org/10.1029/2007GC001805 (n/a–n/a).

Gianni, L., 1971. The Geology of the Belu District of Indonesian Timor. University of London.

Gibbons, A.D., Zahirovic, S., Müller, R.D., Whittaker, J.M., Yatheesh, V., 2015. A tectonic model reconciling evidence for the collisions between India, Eurasia and intra-oceanic arcs of the central-eastern Tethys. Gondwana Research 28, 451–492. http://dx.doi.org/10.1016/j.gr.2015.01.001.

Grady, A.E., Berry, R.F., 1977. Some Palaeozoic–Mesozoic stratigraphic-structural relationships in East Timor and their significance in the tectonics of timor. Journal of the Geological Society of Australia 24, 203–214. http://dx.doi.org/10.1080/00167617708728981.

Haig, D.W., McCartain, E.W., Keep, M., Barber, L., 2008. Re-evaluation of the Cablac Limestone at its type area, East Timor: revision of the Miocene stratigraphy of Timor. Journal of Asian Earth Sciences 33, 366–378. http://dx.doi.org/10.1016/j.jseaes.2008.03.002.

Harley, S.L., Kelly, N.M., Moller, A., 2007. Zircon Behaviour and the Thermal Histories of Mountain Chains. Elements 3, 25–30. http://dx.doi.org/10.2113/gselements.3.1.25.

Harris, R.A., 1991. Temporal distribution of strain in the active Banda orogen: a reconciliation of rival hypotheses. Journal of Southeast Asian Earth Sciences 6, 373–386. http://dx.doi.org/10.1016/0743-9547(91)90082-9.

Harris, R., 2006. Rise and fall of the Eastern Great Indonesian arc recorded by the assembly, dispersion and accretion of the Banda Terrane, Timor. Gondwana Research 10, 207–231. http://dx.doi.org/10.1016/j.gr.2006.05.010.

Harris, R., 2011. The nature of the Banda arc-continent collision in the Timor region. In: Brown, D., Ryan, P.D. (Eds.), Arc-Continent CollisionFrontiers in Earth Sciences. Springer-Verlag, Berlin Heidelberg, pp. 163–211. http://dx.doi.org/10.1007/978-3-540-88558-0_7.

Harris, R.A., Sawyer, R.K., Audley-Charles, M.G., 1998. Collisional melange development: geologic associations of active melange-forming processes with exhumed melange facies in the western Banda orogen, Indonesia. Tectonics 17, 458–479. http://dx.doi.org/10.1029/97TC03083.

Harris, R.A., Kaiser, J., Hurford, A.J., Carter, A., 2000. Thermal history of Australian passive margin sequences accreted to Timor during Late Neogene arc-continent collision, Indonesia. Journal of Asian Earth Sciences 18, 47–69.

Harris, R., Vorkink, M.W., Prasetyadi, C., Zobell, E., Roosmawati, N., Apthorpe, M., 2009. Transition from subduction to arc-continent collision: Geologic and neotectonic evolution of Savu Island, Indonesia. Geosphere 5, 152–171. http://dx.doi.org/10.1130/GES00209.1.

Hunter, D., 1993. A Stratigraphic and Structural Study of the Maubisse area, East Timor, Indonesia.

Kaneko, Y., Maruyama, S., Kadarusman, A., Ota, T., Ishikawa, M., Tsujimori, T., Ishikawa, A., Okamoto, K., 2007. On-going orogeny in the outer-arc of the Timor–Tanimbar region, eastern Indonesia. Gondwana Research 11, 218–233. http://dx.doi.org/10.1016/j.gr.2006.04.013.

Korsch, R.J., Adams, C.J., Black, L.P., Foster, D.A., Fraser, G.L., Murray, C.G., Foudoulis, C., Griffin, W.L., 2009. Geochronology and provenance of the Late Paleozoic accretionary wedge and Gympie Terrane, New England Orogen, eastern Australia⁎. Australian Journal of Earth Sciences. http://dx.doi.org/10.1080/08120090902825776.

Kwon, C.W., Kim, S.W., Park, S.-I., Park, J., Oh, J.-H., Kim, B.C., Koh, H.J., Cho, D.-L., 2014. Sedimentological characteristics and new detrital zircon SHRIMP U–Pb ages of the Babulu Formation in the Fohorem area, Timor-Leste. Australian Journal of Earth Sciences 61, 865–880. http://dx.doi.org/10.1080/08120099.2014.924554.

Lemoine, M., 1959. Un exemple de tectonique chaotique: Timor essai de coordination et d'interpretation. Revue de Géographie Physique et de Géologie Dynamique 2, 205.

Lewis, C.J., Sircombe, K.N., 2013. Use of U-Pb geochronology to delineate provenance of North West Shelf sediments, Australia. In: Keep, M., Moss, S.J. (Eds.), The Sedimentary Basins of Western Australia IV: Proceedings of the Petroleum Exploration Society of Australia Symposium, Perth, WA.

Ludwig, K.R., 2003. User's manual for a geochronological toolkit for Microsoft Excel. Berkeley Geochronol. Cent. Spec. Publ. pp. 1–75.

Major, J.R., 2011. Evolution and emergence of the Hinterland in the active Banda arc-continent collision: insights from the metamorphic rocks and coral terraces of Kisar, Indonesia. Geological Sciences. Brigham Young University, p. vii (38, 63, 55 pp.).

Major, J., Harris, R., Chiang, H.-W., Cox, N., Shen, C.-C., Nelson, S.T., Prasetyadi, C., Rianto, A., 2013. Quaternary hinterland evolution of the active Banda Arc: surface uplift and neotectonic deformation recorded by coral terraces at Kisar, Indonesia. Journal of Asian Earth Sciences 73, 149–161. http://dx.doi.org/10.1016/j.jseaes.2013.04.023.

McCartain, E., Backhouse, J., 2006. Gondwana-related Late Permian palynoflora, foraminifers and lithofacies from the Wailuli Valley. Timor Leste, Neues Jahrbuch fur Geologie und Palaontologie — Abhandlungen 240, 53–80.

McKee, E.H., 1970. Fish Creek Mountains Tuff and volcanic center, Lander County, Nevada. Prof. Pap.

Metcalfe, I., 2002. Permian tectonic framework and palaeogeography of SE Asia. Journal of Asian Earth Sciences 20, 551–566. http://dx.doi.org/10.1016/S1367-9120(02)00022-6.

Metcalfe, I., 2011. Tectonic framework and Phanerozoic evolution of Sundaland. Gondwana Research 19, 3–21. http://dx.doi.org/10.1016/j.gr.2010.02.016.

Metcalfe, I., 2013. Gondwana dispersion and Asian accretion: tectonic and palaeogeographic evolution of eastern Tethys. Journal of Asian Earth Sciences 66, 1–33. http://dx.doi.org/10.1016/j.jseaes.2012.12.020.

Patchett, P.J., 1983. Importance of the Lu–Hf isotopic system in studies of planetary chronology and chemical evolution. Geochimica et Cosmochimica Acta 47, 81–91. http://dx.doi.org/10.1016/0016-7037(83)90092-3.

Patchett, P.J., Tatsumoto, M., 1980. Hafnium isotope variations in oceanic basalts. Geophysical Research Letters 7, 1077–1080. http://dx.doi.org/10.1029/GL007i012p01077.

Prasetyadi, C., Harris, R., 1996. Hinterland structure of the active Banda arc-continent collision, Indonesia: constraints from the Aileu complex of East Timor. Proc. 25th Conv. Indones. Assoc. Geol.

Richardson, A.N., Blundell, D.J., 1996. Continental collision in the Banda arc. Geological Society, London, Special Publications 106, 47–60.

Rosidi, H.M.D., Suwitodirdjo, K., Tjokrosapoetro, S., 1981. Geological Map of the Kupang-Atambua Quadrangle, Timor, scale 1:250.000. Geological Research and Development Centre, Bandung, Indonesia.

Rothpletz, A., 1891. The Permian, Triassic, and Jurassic Formations in the East-Indian Archipelago (Timor and Rotti). American Naturalist 25 (299), 959–962.

Sawyer, R.K., Sani, K., Brown, S., 1993. The stratigraphy and sedimentology of West Timor, Indonesia. Proc. 22nd Conv. Indones. Pet. Assoc, pp. 533–574.

Scherer, E., Münker, C., Mezger, K., 2001. Calibration of the Lutetium-Hafnium Clock. Science 683–687.

Sevastjanova, I., Clements, B., Hall, R., Belousova, E.A., Griffin, W.L., Pearson, N., 2011. Granitic magmatism, basement ages, and provenance indicators in the Malay Peninsula: Insights from detrital zircon U-Pb and Hf-isotope data. Gondwana Research 19, 1024–1039. http://dx.doi.org/10.1016/j.gr.2010.10.010.

Simons, A.L., 1939. Geological investigations in N.E. Netherlands Timor. Geol. Inst. Meded. 85. Univ. of Amsterdam 103 pp.

Söderlund, U., Patchett, P.J., Vervoort, J.D., Isachsen, C.E., 2004. The ^{176}Lu decay constant determined by Lu-Hf and U-Pb isotope systematics of Precambrian mafic intrusions. Earth and Planetary Science Letters 219, 311–324.

Standley, C.E., Harris, R., 2009. Tectonic evolution of forearc nappes of the active Banda arc-continent collision: Origin, age, metamorphic history and structure of the Lolotoi Complex, East Timor. Tectonophysics 479, 66–94. http://dx.doi.org/10.1016/j.tecto.2009.01.034.

Tyler, I.M., Sheppard, S., Bodorkos, S., Page, R.W., 2005. Tectonic significance of detrital zircon age profiles across Palaeoproterozoic orogens in the Kimberley region of northern Australia. In: Wingate, M.T.D., Pisarevsky, S.A. (Eds.), Supercontinents and Earth Evolution Symposium. Geological Society of Australia Inc, Perth, p. 33 Abstracts no. 81).

Please cite this article as: Spencer, C.J., et al., Provenance of Permian–Triassic Gondwana Sequence units accreted to the Banda Arc in the Timor region: Constraints from zircon U–Pb and Hf isotopes, Gondwana Research (2015), http://dx.doi.org/10.1016/j.gr.2015.10.012

van Wyck, N., Willians, I.S., 2002. Age and provenance of basement metasediments from the Kubor and Bena Bena Blocks, central Highlands, Papua New Guinea: constraints on the tectonic evolution of the northern Australian cratonic margin. Australian Journal of Earth Sciences 49, 565–577.

Veevers, J.J., Saeed, A., Belousova, E.A., Griffin, W.L., 2005. U–Pb ages and source composition by Hf-isotope and trace-element analysis of detrital zircons in Permian sandstone and modern sand from southwestern Australia and a review of the paleogeographical and denudational history of the Yilgarn Craton. Earth-Science Reviews 68, 245–279. http://dx.doi.org/10.1016/j.earscirev.2004.05.005.

Vermeesch, P., 2012. On the visualisation of detrital age distributions. Chemical Geology 312–313, 190–194. http://dx.doi.org/10.1016/j.chemgeo.2012.04.021.

Vervoort, J.D., Patchett, P.J., Soderlund, U., Baker, M., 2004. Isotopic composition of Yb and the determination of Lu concentrations and Lu/Hf ratios by isotope dilution using MC-ICPMS. Geochemistry Geophysics Geosystems 5. http://dx.doi.org/10.1029/2004GC000721 Q11002.

Vorkink, M., 2004. Incipient tectonic development of the active Banda arc continent collision : geologic and kinematic evolution of Savu Island, Indonesia MSc. Thesis, Brigham Young University 87 p.

Wang, F., Liu, F., Liu, P., Shi, J., Cai, J., 2014. Petrogenesis of Lincang granites in the south of Lancangjiang area: constrain from geochemistry and zircon U–Pb geochronology. Acta Petrologica Sinica 30, 3034–3050 (in Chinese).

Wanner, J., 1913. Geologie von Westtimor. Geologische Rundschau 4, 136–150. http://dx.doi.org/10.1007/BF01801936.

Wanner, J., 1956. Zur stratigraphie von Portugiesisch Timor. Zeitschrift der Deutschen Geologischen Gesellschaft 108, 109–140.

Williams, H.F., Turner, F.J., Gilbert, C.M., 1982. Petrography, an introduction to the study of rocks in thin section. 2nd ed. W.H. Freeman and Co., San Francisco.

Wopfner, H., Jin, X.C., 2009. Pangea megasequences of Tethyan Gondwana-margin reflect global changes of climate and tectonism in Late Palaeozoic and Early Triassic times - a review. Palaeoworld 18, 169–192.

Woodhead, J., Hergt, J., Shelley, M., Eggins, S., Kemp, R., 2004. Zircon Hf-isotope analysis with an excimer laser, depth profiling, ablation of complex geometries, and concomitant age estimation. Chemical Geology 209, 121–135. http://dx.doi.org/10.1016/j.chemgeo.2004.04.026.

Worden, K.E., Carson, C.J., Scrimgeour, I.R., Lally, J., Doyle, N., 2008. A revised Palaeoproterozoic chronostratigraphy for the Pine Creek Orogen, northern Australia: Evidence from SHRIMP U–Pb zircon geochronology. Precambrian Research 166, 122–144.

Zobell, E.A., 2007. Origin and Tectonic Evolution of Gondwana Sequence Units Accreted to the Banda Arc: A Structural Transect through Central East Timor. Unpublished M.S. Thesis, Brigham Young University.

Please cite this article as: Spencer, C.J., et al., Provenance of Permian–Triassic Gondwana Sequence units accreted to the Banda Arc in the Timor region: Constraints from zircon U–Pb and Hf isotopes, Gondwana Research (2015), http://dx.doi.org/10.1016/j.gr.2015.10.012